THE ANALYTICAL MECHANICS OF THE GYROSCOPE IN ECE2 THEORY

by

M. W. Evans and H. Eckardt

Civil List and AIAS / UPITEC

(www.aias.us, www.upitec.org, www.et3m.net, www.archive.org, www.webarchive.co.uk)

ABSTRACT

The analytical mechanics of the gyroscope are worked out exactly with a numerical method, and applied to the demonstration by Laithwaite that a gyroscope held at arm's length above the surface of the earth appears to be weightless. The solution is worked out in terms of torques in the laboratory frame (X, Y, Z) and the frame of the principal moments of inertia (1, 2, 3). The extra effects of the convective derivative of ECE2 theory are discussed.

Keywords: ECE2 theory, analytical mechanics of the gyroscope.

UFT 368

1. INTRODUCTION

The preceding paper initiated the development of the well known {1 - 12} analytical mechanics of a gyroscope with the aim of explaining a replicated experiment by Laithwaite in which it was demonstrated that a spinning wheel held at arms length on a horizontal axis above the earth's surface appears to be weightless. In Section 2 the problem is analyzed in terms of three Euler Lagrange equations in the three Euler angles. These are three simultaneous differential equations which are solved numerically to give the complete analytical mechanics of the gyroscope. The method considers any laboratory frame torque applied to the gyroscope.

This paper is a brief synopsis of detailed calculations found in the notes accompanying UFT368 on www.aias.us. These notes should be read with the paper. Note 368(1) describes constants of motion for the motion of the centre of mass of the gyroscope. Notes 368(2) to 368(5) consider anew the example of a symmetric top with one point fixed, first considered by Lagrange in "Mecanique Analytique" (1811 and 1815). Notes 368(6) to 368(8) are the basis for Section 2 and provide a complete solution to the problem using the program Maxima combined with analysis. The Laithwaite experiment is an example of the complete solution.

2. DEFINITION AND SOLUTION OF THE PROBLEM.

Consider the definition of the torque in analytical mechanics (classical dynamics):

$$\underline{Tq}_{(XYZ)} = \left(\frac{d\underline{L}}{dt}\right)_{(XYZ)} = \left(\frac{d\underline{L}}{dt} + \underline{\omega} \times \underline{L}\right)_{(123)} \quad -(1)$$

Here $\underline{L}$ is the angular momentum and the subscript 123 denotes the frame defined by the principal moments of inertia of the gyroscope. The laboratory frame is denoted (X, Y, Z). The well known Euler equations follow from Eq. (1):

$$Tq_1 = I_1\dot{\omega}_1 - (I_2 - I_3)\,\omega_2\omega_3 \quad -(2)$$
$$Tq_2 = I_2\dot{\omega}_2 - (I_3 - I_1)\,\omega_3\omega_1 \quad -(3)$$
$$Tq_3 = I_3\dot{\omega}_3 - (I_1 - I_2)\,\omega_1\omega_2. \quad -(4)$$

Here $\omega_1, \omega_2, \omega_3$ are the principal angular velocities in frame (1, 2, 3) and where I_1, I_2, and I_3 are the three principal moments of inertia of the gyroscope. In terms of the well known Euler angles θ, ϕ, χ {1 - 12}:

$$\omega_1 = \dot{\phi}\sin\theta\sin\chi + \dot{\theta}\cos\chi \quad -(5)$$
$$\omega_2 = \dot{\phi}\sin\theta\cos\chi - \dot{\theta}\sin\chi \quad -(6)$$
$$\omega_3 = \dot{\phi}\cos\theta + \dot{\chi}. \quad -(7)$$

It follows that:

$$\dot{\omega}_1 = \frac{d}{dt}\left(\dot{\phi}\sin\theta\sin\chi + \dot{\theta}\cos\chi\right) \quad -(8)$$
$$\dot{\omega}_2 = \frac{d}{dt}\left(\dot{\phi}\sin\theta\cos\chi - \dot{\theta}\sin\chi\right) \quad -(9)$$
$$\dot{\omega}_3 = \frac{d}{dt}\left(\dot{\phi}\cos\theta + \dot{\chi}\right). \quad -(10)$$

Note carefully that:

$$\theta = \theta(t), \quad \phi = \phi(t), \quad \chi = \chi(t), \quad -(11)$$

so if for example:

$$y = \cos\theta(t) \quad -(12)$$

then:

$$\frac{dy}{dt} = \frac{dy}{d\theta}\frac{d\theta}{dt} = -\dot{\theta}\sin\theta \quad -(13)$$

and so on.

Therefore as in Note 368(8):

$$\dot{\omega}_1 = \ddot{\phi}\sin\theta\sin\psi + \dot{\phi}\left(\dot{\theta}\sin\psi\cos\theta + \dot{\psi}\sin\theta\cos\psi\right) + \ddot{\theta}\cos\psi - \dot{\theta}\dot{\psi}\sin\psi$$

$$\dot{\omega}_2 = \ddot{\phi}\sin\theta\sin\psi + \dot{\phi}\left(\dot{\theta}\sin\psi\cos\theta + \dot{\psi}\sin\theta\cos\psi\right) - \ddot{\theta}\sin\psi + \dot{\theta}\dot{\psi}\cos\psi$$

$$\dot{\omega}_3 = \ddot{\phi}\left(\cos\theta - \dot{\theta}\sin\theta\right) + \ddot{\psi}. \quad -(14)$$

The lagrangian of the gyroscope was first defined by Lagrange in "Mecanique Analytique" in 1811 and 1815:

$$\mathcal{L} = T - U \quad -(15)$$

where the kinetic energy is:

$$T = \frac{1}{2}I_{12}\left(\dot{\phi}^2\sin^2\theta + \dot{\theta}^2\right) + \frac{1}{2}I_3\left(\dot{\phi}\cos\theta + \dot{\psi}\right)^2 \quad -(16)$$

and the potential energy is

$$U = mgh\cos\theta. \quad -(17)$$

The mass of the gyroscope is m, g is the magnitude of the acceleration due to gravity, and h is the constant distance between the origin and the centre of mass. The origins of frames (1, 2, 3) and (X, Y, Z) coincide. The gyroscope is considered to be a symmetric top, so two moments of inertia are the same and denoted by:

$$I_{12} = I_1 = I_2 \quad -(18)$$

The three Euler Lagrange equations in the three Euler angles are:

$$\frac{\partial \mathcal{L}}{\partial \theta} = \frac{d}{dt}\frac{\partial \mathcal{L}}{\partial \dot{\theta}} \quad -(19)$$

$$\frac{\partial \mathcal{L}}{\partial \phi} = \frac{d}{dt}\frac{\partial \mathcal{L}}{\partial \dot{\phi}} \quad -(20)$$

$$\frac{\partial \mathcal{L}}{\partial \psi} = \frac{d}{dt}\frac{\partial \mathcal{L}}{\partial \dot{\psi}} \quad -(21)$$

from which two constants of motion can be defined:

$$L_\phi = \frac{\partial \mathcal{L}}{\partial \dot{\phi}} = (I_{12}\sin^2\theta + I_3\cos^2\theta)\,\dot{\phi} + I_3\dot{\psi}\cos\theta \quad -(22)$$

$$L_\psi = \frac{\partial \mathcal{L}}{\partial \dot{\psi}} = I_3(\dot{\psi} + \dot{\phi}\cos\theta). \quad -(23)$$

These are constant angular momenta which do not change with time:

$$dL_\phi / dt = 0, \quad -(24)$$

$$dL_\psi / dt = 0. \quad -(25)$$

It follows that {1 - 12}:

$$\dot{\phi} = \frac{L_\phi - L_\psi\cos\theta}{I_{12}\sin^2\theta} \quad -(26)$$

and

$$\dot{\psi} = \frac{1}{I_3}\left(L_\psi - I_3\dot{\phi}\cos\theta\right) \quad -(27)$$

The Euler Lagrange equation (19) gives the result:

$$\ddot{\theta} = \frac{\sin\theta}{I_{12}}\left(\dot{\phi}^2\cos\theta\,(I_{12} - I_3) - I_3\dot{\phi}\dot{\psi} + mgh\right) \quad -(28)$$

Eqs. (26), (27) and (28) are three simultaneous differential equations which must be solved to give the trajectories of the three Euler angles. This solution is carried out numerically and without approximation in this paper using Maxima. The results are graphed in Section 3 and show well defined nutation and precession. This appears to be the first time that an exact solution of gyroscope dynamics has been found. All previous solutions, including that of Lagrange, are necessarily approximate, because the motion of the gyroscope is very intricate.

Therefore the three torque components of frame (1, 2, 3) can be found from the trajectories of the Euler angles and from $\dot{\theta}, \dot{\phi}, \dot{\psi}, \ddot{\theta}, \ddot{\phi}, \ddot{\psi}$. This calculation is carried out by computer algebra. It is not possible by hand beca e of the complexity of the problem. The complete solution reveals features of gyroscope motion which are hitherto unknown.

The complete moving frame torque is:

$$\underline{Tq} = Tq_1 \underline{e}_1 + Tq_2 \underline{e}_2 + Tq_3 \underline{e}_3 \quad -(29)$$

where $\underline{e}_1, \underline{e}_2, \underline{e}_3$ are unit vectors in the (1, 2, 3) frame. The torque in the laboratory frame is:

$$\underline{Tq} = \underline{r} \times \underline{F} = Tq_X \underline{i} + Tq_Y \underline{j} + Tq_Z \underline{k} \quad -(30)$$

and the two torques are related by Eq. (1). We consider $\underline{F}$ to be the force of gravity on the centre of mass of the gyroscope:

$$\underline{F} = mg\underline{k}. \quad -(31)$$

In general:

$$\underline{r} = X\underline{i} + Y\underline{j} + Z\underline{k} \quad -(32)$$

so:

$$\underline{Tq} = \begin{vmatrix} \underline{i} & \underline{j} & \underline{k} \\ X & Y & Z \\ 0 & 0 & mg \end{vmatrix} = mg\left(Y\underline{i} - X\underline{j}\right). \quad -(33)$$

The origins of (X, Y, Z) and (1, 2, 3) are the same, so:

$$Tq_X^2 + Tq_Y^2 + Tq_Z^2 = Tq_1^2 + Tq_2^2 + Tq_3^2 = m^2g^2\left(Y^2 + X^2\right). \quad -(34)$$

In the symmetric top with one point fixed:

$$X^2 + Y^2 = h^2 \quad -(35)$$

so

$$Tq_1^2 + Tq_2^2 + Tq_3^2 = m^2g^2h^2. \quad -(36)$$

Therefore:

$$F^2 = \frac{1}{h^2}\left(Tq_1^2 + Tq_2^2 + Tq_3^2\right). \quad -(37)$$

The force of gravitation is attractive and negative valued:

$$\underline{F} = mg\underline{k} = -\frac{mMG}{R^2}\underline{k} \quad -(38)$$

where M is the mass of the earth and R is its radius. Therefore:

$$g = -\frac{MG}{R^2}. \quad -(39)$$

In the gyroscope the force of gravity is countered by the positive valued force magnitude:

$$F = \frac{1}{h}\left(Tq_1^2 + Tq_2^2 + Tq_3^2\right)^{1/2} \quad -(40)$$

If a gyroscope is perceived to be weightless in the Laithwaite configuration, then:

$$|mg| = \frac{1}{h}\left(Tq_1^2 + Tq_2^2 + Tq_3^2\right)^{1/2} \quad -(41)$$

Other laboratory frame torques can be considered in this problem, for example an applied mechanical torque that results in an additional force in the positive $\underline{k}$ direction of the laboratory frame, and also the convective torque of ECE2 theory:

$$\underline{Tq}\,(\text{convective}) = \left(\underline{v}\cdot\underline{\nabla}\right)\underline{L} \quad -(42)$$

which acts in the laboratory frame and which is a small vacuum correction, the vacuum being considered to be a fluid.

3. NUMERICAL SOLUTION AND GRAPHICAL ANALYSIS.

(Section by Dr Horst Eckardt)

The analytical mechanics of the gyroscope in ECE2 theory

M. W. Evans[*], H. Eckardt[†]
Civil List, A.I.A.S. and UPITEC

(www.webarchive.org.uk, www.aias.us,
www.atomicprecision.com, www.upitec.org)

3 Numerical solution and graphical analysis

The equations of motion (26-28) for the Euler angles θ, ϕ, ψ have been solved numerically. The result is the motion of the centre of mass, transformed to cartesian coordinates:

$$\mathbf{R} = \begin{bmatrix} X \\ Y \\ Z \end{bmatrix} = \begin{bmatrix} h \sin\theta \cos\phi \\ h \sin\theta \sin\phi \\ h \cos\theta \end{bmatrix} \tag{43}$$

in dependence of time. The angular velocities of the principal axes of the rigid body have been given by Eqs. (5-7). ω_3 is a constant of motion and can be expressed by

$$\omega_3 = \frac{L_\psi}{I_3}. \tag{44}$$

The numerical results were obtained for the first data set (in SI units):

$$\begin{aligned} I_{12} &= 0.5 \\ I_3 &= 4 \\ L_\phi &= 1 \\ L_\psi &= 3.8 \\ m &= 10 \\ g &= 9.81 \\ h &= 0.2 \end{aligned} \tag{45}$$

In this case we have $L_\phi < L_\psi$, it is a slowly precessing gyro with momentum of inertia mainly in x_3 body axis. The gyro has a typical "thick" rotor with

*email: emyrone@aol.com
†email: mail@horst-eckardt.de

$I_{12} < I_3$. Initial values for the calculation were

$$\begin{aligned}
\dot{\theta}_0 &= 0 \\
\theta_0 &= \pi/4 \\
\phi_0 &= \pi/4 \\
\psi_0 &= 0
\end{aligned} \tag{46}$$

It should be noted that it is not possible to define an initial precession speed, this is completely determined by the equations which are of first time order in ϕ and ψ. Results for the above data set (45) are shown in the first five figures. Fig. 1 presents the nutation angle θ and its angular velocity, both are nearly harmonic. From Fig. 2 can be seen that ϕ increases linearly but with small oscillations. ψ has a more complex substructure. The oscillations in ϕ lead to a meandering motion of the centre of mass composed by precession and nutation which is graphed in a space curve in Fig. 3. The velocity components ω_1, ω_2 in body coordinates (Fig. 4) show oscillating behaviour while ω_3 is constant as mentioned above. Graphed as a space curve, this gives a rosette-like motion, see Fig. 5.

In the next set of numerical calculations we have exchanged the angular momenta:

$$\begin{aligned}
L_\phi &= 3.8 \\
L_\psi &= 1
\end{aligned} \tag{47}$$

with other parameters taken as before. Now the behaviour of ϕ and ψ has interchanged (Fig. 6). The precession is faster due to the higher angular momentum L_ϕ and there is less variation as can be seen from the spacecurve Fig. 7. The components of angular velocity (Fig. 8) have a larger period with some overlaid smaller structure. Their vector now describes a circle with sharp oscillations, see Fig. 9.

Finally we tried to mimic the behaviour of a free falling gyro in a simple way. Assuming that the gravitational force is counteracted by a force of motion as in Laithwaite's experiment, we replace the mass m in the potential energy term (17) by a difference of effective masses:

$$U = (m - m_1)\ g\ h\ \cos\theta.$$

m_1 is a "counter-mass" simulating the lifting of the gyro. In case of $m = m_1$, there is no potential energy term. The only place where this enters the computation is in Eq. (28). So omitting this term gives interesting results. Using the first data set (45), the angles ϕ and ψ (Fig. 10) look similar as before (Fig. 2) but there is no progression of the precession, ϕ oscillates constantly in the low angular range. What this means can be seen from the space curve of centre of mass (Fig. 11). The mass rotates periodically in an elliptic motion. Consequently, the angular velocity components are strictly periodic (Fig. 12) and their space curve describes a circle with constant height (Fig. 13), due to the constant ω_3 component. This is a quite unexpected behaviour, showing that a symmetric top with one point fixed only gives precessional motion when an external force is present. The precession is a result of gravity. The complete Lagrangian description of a free floating spinning top will be investigated in UFT paper 369.

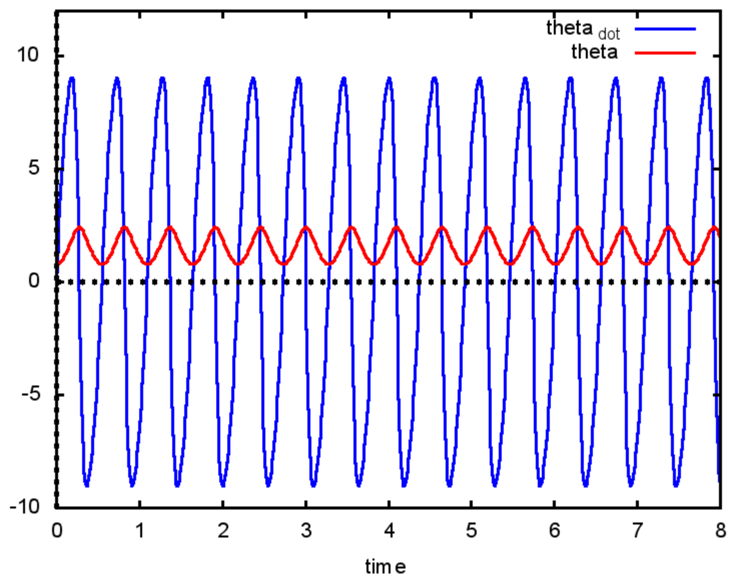

Figure 1: Angular velocity $\dot{\theta}$ and angle of nutation θ.

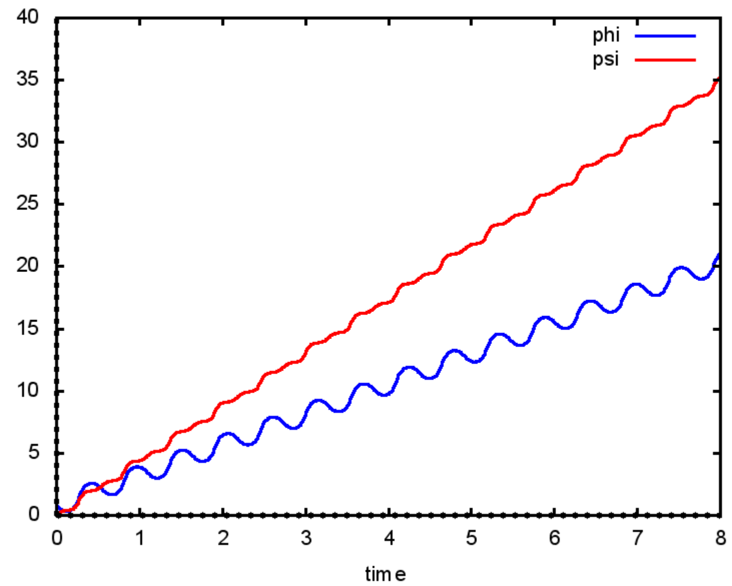

Figure 2: Angle of precession ϕ and Euler angle ψ.

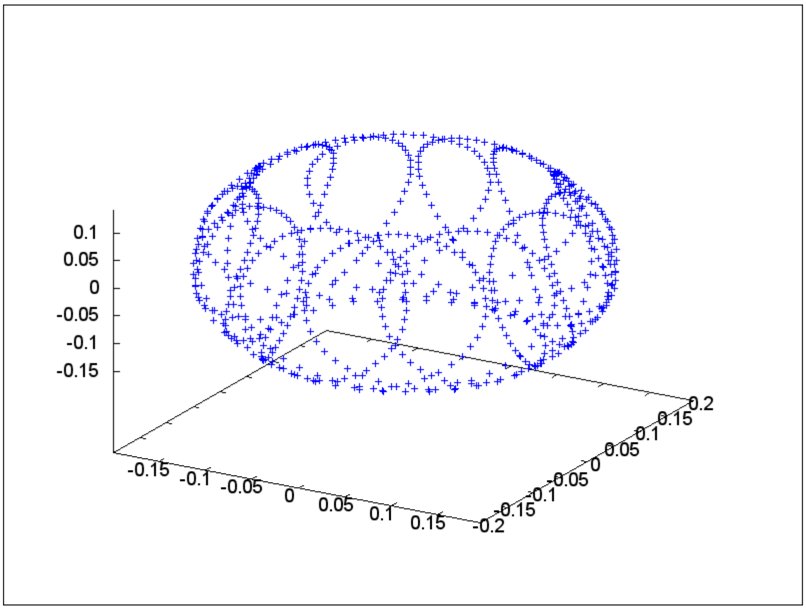

Figure 3: Space curve of centre of mass motion **R**.

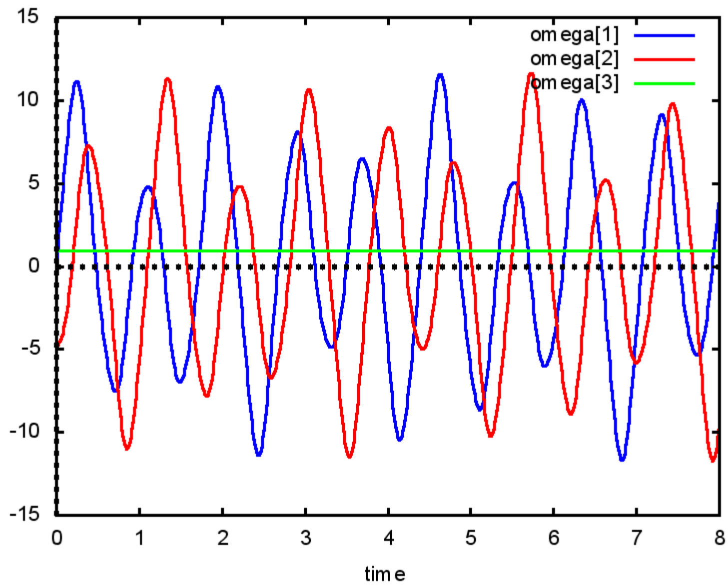

Figure 4: Angular velocity components of $\boldsymbol{\omega}$ in body coordinates.

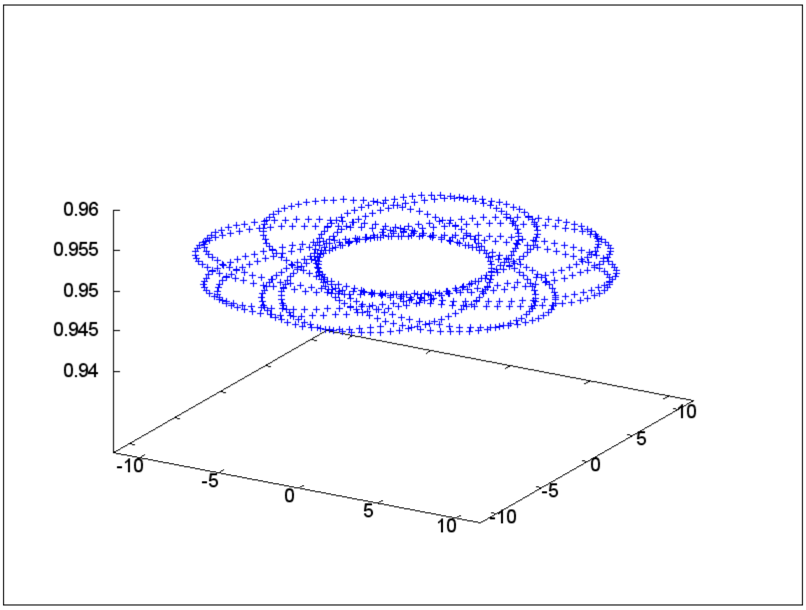

Figure 5: Space curve of angular velocity $\boldsymbol{\omega}$ in body coordinates.

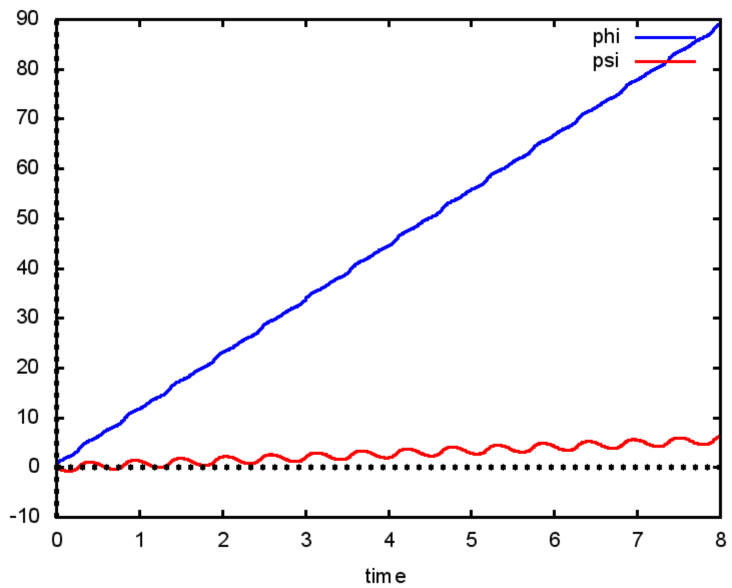

Figure 6: Angle of precession ϕ and Euler angle ψ, second data set.

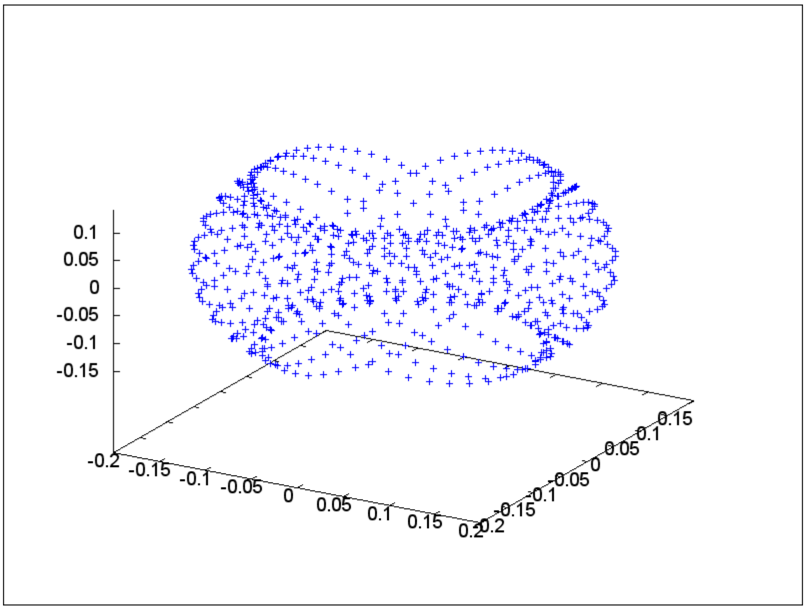

Figure 7: Space curve of centre of mass motion $\mathbf{R}$, second data set.

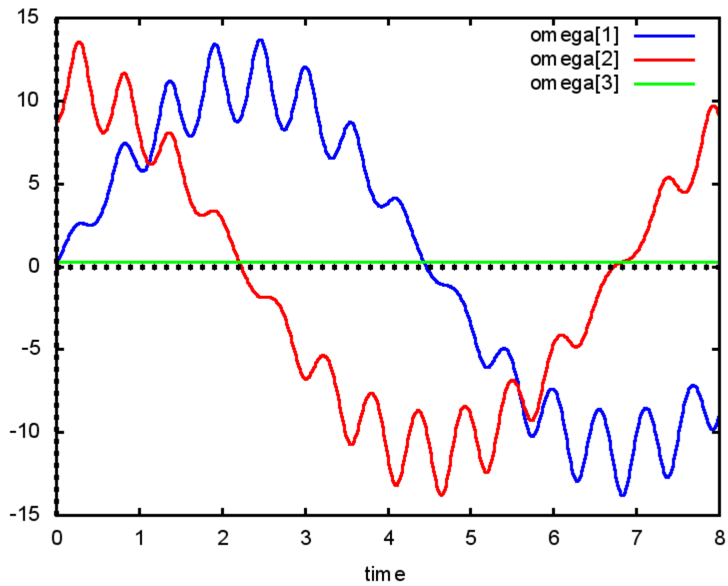

Figure 8: Angular velocity components of $\boldsymbol{\omega}$ in body coordinates, second data set.

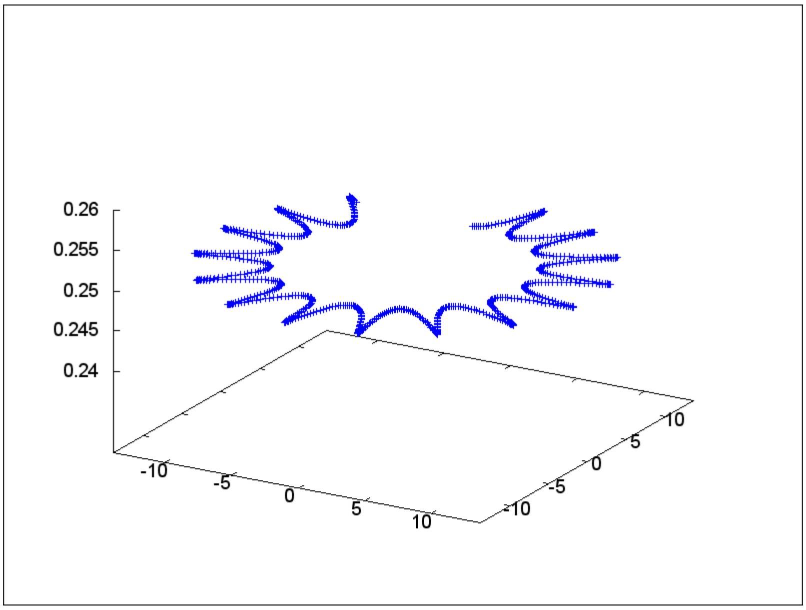

Figure 9: Space curve of angular velocity $\boldsymbol{\omega}$ in body coordinates, second data set.

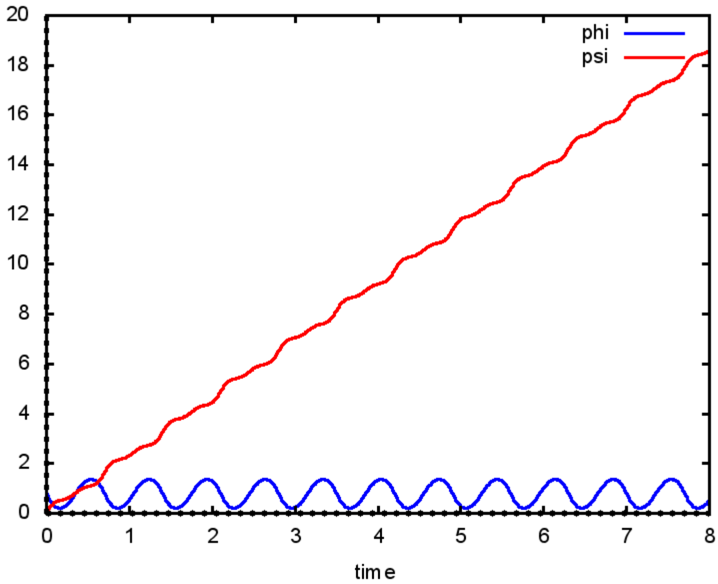

Figure 10: Angle of precession ϕ and Euler angle ψ, weightless gyro.

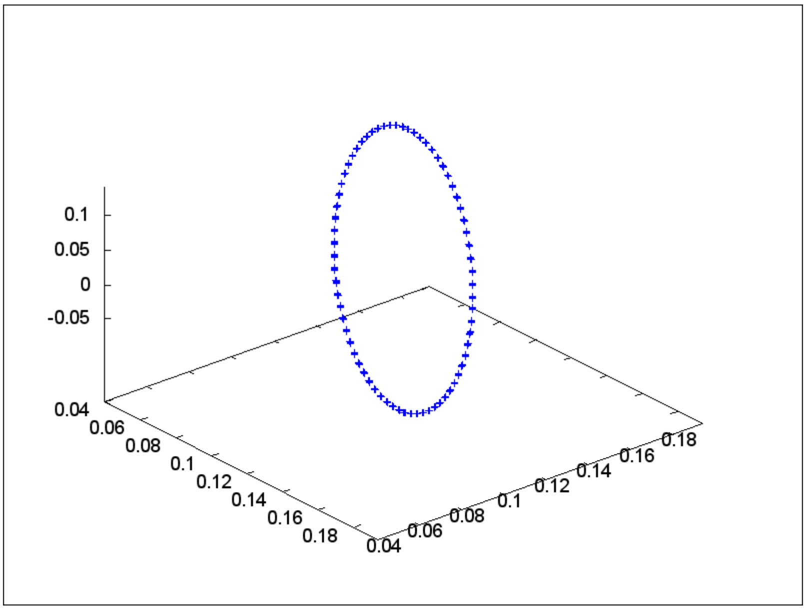

Figure 11: Space curve of centre of mass motion $\mathbf{R}$, weightless gyro.

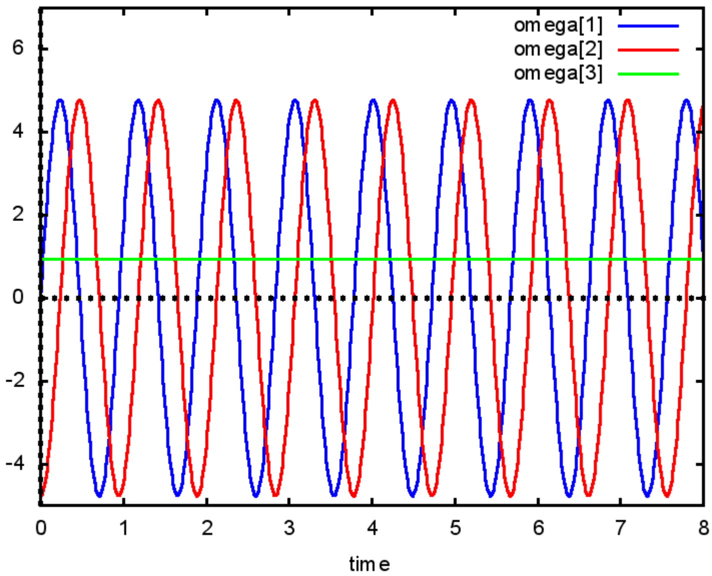

Figure 12: Angular velocity components of $\boldsymbol{\omega}$ in body coordinates, weightless gyro.

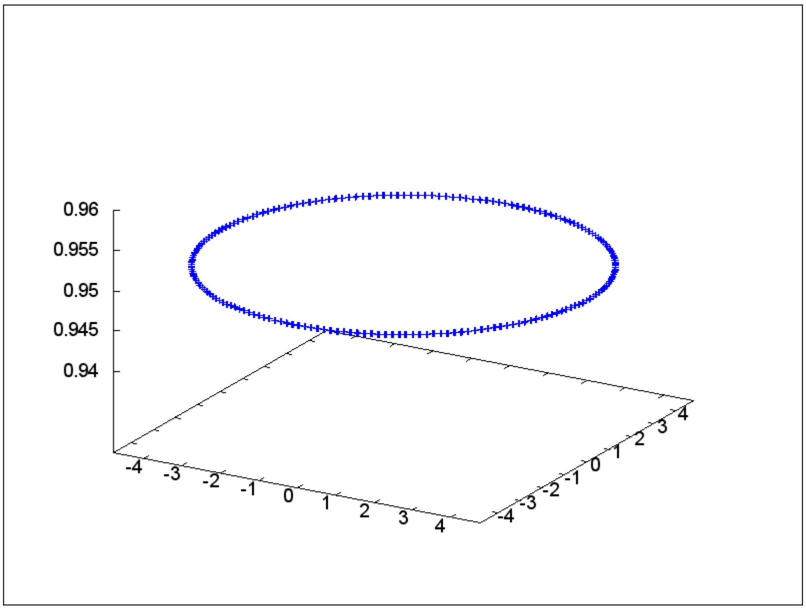

Figure 13: Space curve of angular velocity $\boldsymbol{\omega}$ in body coordinates, weightless gyro.

ACKNOWLEDGMENTS

The British Government is thanked for a Civil List Pension and the staff of AIAS and others for many interesting discussions. Dave Burleigh is thanked for voluntary posting, site maintenance and hosting of www.aias.us and feedback software and hardware maintenance. Alex Hill is thanked for translation and broadcasting, and Robert Cheshire for broadcasting.

REFERENCES

{1} M. W. Evans, H. Eckardt, D. W. Lindstrom and S. J. Crothers, "ECE2: The Second Paradigm Shift" (UFT366 and Spanish Section of www.aias.us, www.upitec.org , and Epubli, Berlin, 2017 in prep., translation by Alex Hill).

{2} M .W. Evans, H. Eckardt, D. W. Lindstrom and S. J. Crothers, "The Principles of ECE" (UFT350, Spanish and publications section of www.aias.us, www.upitec.org, Epubli Berlin 2016 (hardback) and New Generation, London, 2016 (softback), translation by Alex Hill).

{3} M .W. Evans, S. J. Crothers, H. Eckardt and K. Pendergast, "Criticisms of the Einstein Field Equation" (UFT301 and Cambridge International (CISP), 2010).

{4} L. Felker, "The Evans Equations of Unified Field Theory" (Abramis 2007 and UFT302, Spanish translation by Alex Hill).

{5} H. Eckardt, "The ECE Engineering Model" (UFT303).

{6} M. W. Evans, "Collected Scientometrics" (UFT307 and filtered statistics of www.aias.us).

{7} M .W. Evans, H. Eckardt and D. W. Lindstrom, "Generally Covariant Unified Field Theory" (Abramis 2005 to 2011 and relevant UFT papers on www.aias.us and www.upitec.org) in seven volumes softback.

{8} M .W. Evans and L. B. Crowell, "Classical and Quantum Electrodynamics and the B(3) Field" (World Scientific, 2001, Omnia Opera section of www.aias.us).

{9} M .W. Evans and S. Kielich (eds.), "Modern Nonlinear Optics" (Wiley Interscience, New York, 1992, 1993, 1997 and 2001) in two editions and six volumes.

{10} M. W. Evans, Ed. J. Found. Phys. Chem. (CISP 2011 and relevant UFT papers).

{11} M. W. Evans and J.- P. Vigier, "The Enigmatic Photon" (Kluwer 1994 to 2002 and Omnia Opera Section of www.aias.us) in five volumes hardback and five volumes softback.

{12} M .W. Evans and A. A. Hasanein, "The Photomagneton in Quantum Field Theory" (World Scientific 1994)